Solid-State Electronics Vol. 21, pp. 1519–1524

0038-1101/78/1201-1519/$02.00/0

SCANNING PHOTOCURRENT MICROSCOPY: A NEW TECHNIQUE TO STUDY INHOMOGENEOUSLY DISTRIBUTED RECOMBINATION CENTERS IN SEMICONDUCTORS

DAVID V. LANG and CHARLES H. HENRY
Bell Laboratories, Murray Hill, NJ 07974, U.S.A.

Abstract—We report a new method of recombination-center microscopy which is based on the well known steady-state junction photocurrent measurements. In this technique photocurrent is generated by optical excitation of deep levels using a laser having an energy less than the energy gap. An x–y laser scan across the sample is displayed on a CRT. The intensity of the CRT is modulated by the photocurrent signal. We discuss the basic physics of the photocurrent genration process as well as the operating characteristics of the scanning system. Examples are given for the case of catastrophic degradation and classic (100) dark-line defects in GaAs/$Al_xGa_{1-x}As$ double heterojunctions. Finally, we discuss the relative merits of this technique as compared to other methods of recombination microscopy.

NOTATION

σ'' optical cross section, cm^2
v_t carrier thermal velocity, cm/sec
τ recombination lifetime of bound carrier, sec
σ_n electron capture cross section, cm^2
$h\nu$ photon energy, eV
E_g energy gap, eV
S laser photon flux, $cm^{-2}\,sec^{-1}$.

1. INTRODUCTION

It has become increasingly clear in recent years that nonradiative recombination centers in semiconductors may be spatially distributed in a very inhomogeneous fashion. A prime example is the well known dark-line defect (DLD) which may be generated during the operation of a semiconductor laser or LED. These defects have been shown to be composed of a complex network of dislocations which grows by a climb process stimulated by nonradiative recombination in the vicinity of the DLD[1–4]. The simplest way to obtain information about the inhomogeneous nature of such defects is to form an image in an optical microscope of the band-gap luminescence from the sample, using either forward-bias injection[5] or optical injection[6] of excess minority carriers. In such an image the nonradiative defect appears dark because the luminescence efficiency is locally reduced near the defect. It is also possible to image the below-band-gap luminescence associated with emission from inhomogeneously distributed defects[7, 8]. In cases where the luminescence is not in the visible range, one typically employs an IR image converter.

Various techniques using a scanning electron microscope (SEM) have also been developed for studying inhomogeneously distributed nonradiative (or radiative) defects. The simplest method is to measure the decrease in the electron-beam-induced current (EBIC) in the vicinity of a nonradiative defect near a *pn* junction or Schottky barrier[9–11]. The same information may be obtained from the decrease in the electron-beam-induced luminescence (cathodoluminescence) in the vicinity of the defect[10, 11]. It is also possible to use a scanning *laser* beam, instead of a scanning *electron* beam, to obtain information about the spatial distribution of recombination centers in semiconductors[12–14]. This is exactly analogous to the SEM EBIC case where the changes in the short-circuit photocurrent[14] or open-circuit photovoltage[12, 13] are used to form an image of the distribution of recombination centers in the sample. In both the SEM and scanning laser techniques, the measured signal is used to modulate the intensity of CRT display which is scanned in synchronism with the electron or laser beam.

Nearly all of the above techniques have in common the measurement of quantity associated with the *minority-carrier* concentration. Thus a region of locally high recombination-center density is manifested by a local reduction in the minority-carrier lifetime which leads to a reduction in such properties such as photocurrent or band-edge luminescence. Recently, an effort has been made to obtain direct information about the localized recombination regions by developing forms of recombination microscopy which are based on the optical or thermal-emission properties of the defect. These techniques make use of the various spectroscopic methods which have been widely used to study the properties of deep-level defects without regard to their spatial location. We have already mentioned one example, namely, the direct imaging of deep-level luminescence[7, 8]. One can also consider the application of various forms of junction space-charge spectroscopy to recombination microscopy. Recently, the technique of deep-level transient spectroscopy (DLTS)[15] has been adapted for use in a modified SEM to obtain the thermal-emission spectrum and spatial distribution of recombination centers near *pn* junctions or Schottky barriers[11, 16]. This is called scanning DLTS (SDLTS). In this paper we will discuss the extension of junction

photocurrent methods[17–20] to the study of the spatial distribution of recombination centers.

2. BASIC PHYSICS OF JUNCTION PHOTOCURRENT

The junction photocurrent techniques[17–20] are based on the same principle as bulk photoconductivity, namely, the optical emission of carriers from deep levels. In the junction case, however, the analysis is considerably simplified since the emitted carriers are rapidly swept out of the junction space-charge region so that retrapping effects can be neglected. The spectral response of the steady state junction photocurrent can be related to the optical emission cross sections of the center and thus in principle provide information similar to that obtained by optical absorption measurements. In practice, however, it is often difficult to deconvolute the steady-state photocurrent spectrum without additional information. This spectrum is nonetheless a useful "fingerprint" of the defect, especially when coupled with the spatial information possible with the X-Y scanning technique to be discussed here.

The photocurrent density generated within the space-charge region due to a particular deep level is given by[19, 20]

$$J = qN_T \left(\frac{\sigma_n^o \sigma_p^o}{\sigma_n^o + \sigma_p^o} \right) S(W - W_o) \qquad (1)$$

where N_T is the density of deep levels, σ_n^o and σ_p^o are the optical cross sections for photoionization of electrons and holes, $S = P/h\nu$ is the photon flux of the laser, P is the laser power density, W is the total width of the space-charge layer, and W_o is the effective width of the edge regions of the space-charge layer where carrier capture dominates over optical emission[19, 20]. Equation (1) is an expression valid at low light intensities when only levels within the space-charge layer contribute to the photocurrent. For sufficiently high laser intensities, minority carriers generated at levels existing *outside* the space-charge layer but within a diffusion length of the junction will contribute. Such a diffusion current will be generated only when $\sigma^o S\tau \geq 1$, where $\sigma^o S$ is the rate of excitation of minority carriers from the deep level to the band and τ is the lifetime for the bound carrier to recombine. Let us consider a set of typical parameters: $\sigma^o = 10^{-16}$ cm^2, $S = 2 \times 10^{23}$ photons cm^{-2} sec^{-1} and (the flux of a 1 mW laser beam focused to a 1.5 μm on diameter spot size) $\tau = (\sigma_n v n)^{-1}$ where $v = 2 \times 10^7$ cm/sec and $n = 10^{17}$ cm^{-3}. Under these conditions $\sigma^o S\tau$ is greater than unity only if $\sigma_n < 10^{-17}$ cm^{-2}. This is a rather small capture cross section. We might expect[22] typical efficient nonradiative centers to have capture cross sections in the range 10^{-16}–10^{-14} cm^2. Thus it is unlikely that the centers in the examples to be shown later in this paper would be in the high-excitation limit. One must take care to analyze each case separately, however, since for lower carrier concentrations and/or higher laser powers one might easily be in this regime. The onset on the high-excitation limit can be recognized by a super-linear dependence of the photocurrent on laser intensity as the diffusion current starts to become important.

3. LASER SCANNING SYSTEM

The laser scanning system is similar to that used for above-band-gap photocurrent[14] and photovoltage[12, 13] imaging. A schematic diagram of the experimental set-up is shown in Fig. 1. The optimal laser wavelength depends on the band-gap of the host material and on the type of measurement desired. Ideally one would like a tunable laser so that one could obtain the photocurrent lineshape. Since a two-step excitation (from the valence band to the deep level and from the deep level to the conduction band) is necessary for steady-state photocurrent, one is limited with a given laser photon energy $h\nu$ to detecting deep levels in a region of energy $2h\nu - E_g$ wide in the center of the gap. Thus if $h\nu = E_g/2$, one could detect the steady state photocurrent *only* from levels exactly at mid-gap. At the opposite extreme, a laser for which $h\nu = E_g$ would detect all deep levels in the gap. For studies of GaAs (E_g = 1.4 eV at room temperature) we have used either a 1.06-μm Nd-YAG laser or a 1.15-μm He–Ne laser for sub-band-gap measurements, and a 6328 Å He–Ne laser for above-band-gap measurements.

The scanning mirrors and their controls in Fig. 1 are standard, commercially available components[23]. The lens is a high-quality microscope objective. The minimum focussed laser spot diameter for a ×40, 0.6 NA lens, as measured by the 20%–80% points on the signal fall-off at a cleaved edge of the sample, is $\approx$1.3 μm for the 1.06 μm laser and $\approx$2.0 μm for the 6328 Å laser. The laser output was typically attenuated by neutral density filters to be in the range of 1–10 mW. Typical photocurrents were 0.01–1.0 μA. These are amplified by a current amplifier and the resulting signal applied to "z-axis" intensity control of an oscilloscope with a persistent-phosphor CRT. The extrinsic photocurrent image can then be formed when the oscilloscope is rastered in synchronism with the mirrors. In practice this is

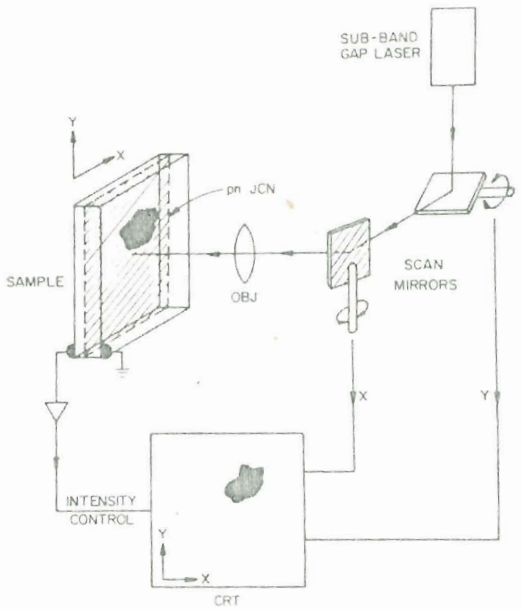

Fig. 1. Schematic diagram of scanning extrinsic photocurrent microscope.

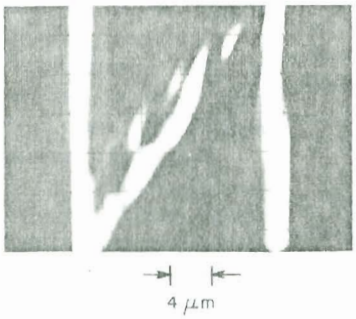

Fig. 3. Scanning extrinsic photocurrent image of a classical (100) dark-line defect in a photon-bombarded stripe-geometry $GaAs/Al_xGa_{1-x}As$ DH laser. The vertical bright lines define the edges of the DH laser stripe which is imaged by scanning the microscope laser beam in the x-y plane of the active epitaxial layer.

achieved by simply applying the voltage-ramp output signals from the mirror scanning control units to the x- and y-axes of the oscilloscope. A *line scan* is formed for a fixed value of y, for example, by applying the photocurrent signal to the vertical axis of the oscilloscope and the x-axis mirror-scanning ramp to the horizontal axis. The operation of this scanning photocurrent microscope is thus *exactly* analogous to that of a scanning electron microscope in the EBIC mode. The physical origin of the sub-band-gap photocurrent is quite different, however.

4. TYPICAL RESULTS

To illustrate the operation of the scanning photocurrent microscope we will consider here its application to localized nonradiative defects in two systems. Namely: (1) the case of catastrophic degradation of $GaAs/Al_xGa_{1-x}As$ double heterostructure (DH) *pn* junctions induced by intense pulsed optical excitation[24], and (2) the case of classic (100) DLDs in $GaAs/Al_xGa_{1-x}As$ DH stripe-geometry lasers[1–6].

The first example is shown in Fig. 2. This is a line scan across three catastrophically induced dark lines, labelled *D*. The above-band-gap photocurrent scan obtained with the 6328 Å laser shows a *decrease* in the collected current at these defects. A similar effect is seen in these samples with the SEM EBIC or cathodoluminescence mode[11, 24]. The below-band-gap 1.06 μm laser scan in the lower part of Fig. 2 shows sharp *increases* in the photocurrent corresponding to these defects. The irregular background of the 6328 Å scan is clearly not due to recombination centers in this case. It is due to multiple-reflection interferrence effects in the 0.5-μm-thin $Al_{0.8}Ga_{0.2}As$ top layer of this sample which is transparent to the 6328 Å light. The below-band-gap 1.06 μm photocurrent signal in Fig. 2 demonstrates that nonradiative recombination at the dark lines is due to a large concentration of point defects. The defects are quenched into the crystal by local melting followed by rapid recrystalization that occurs during catastrophic degradation[24].

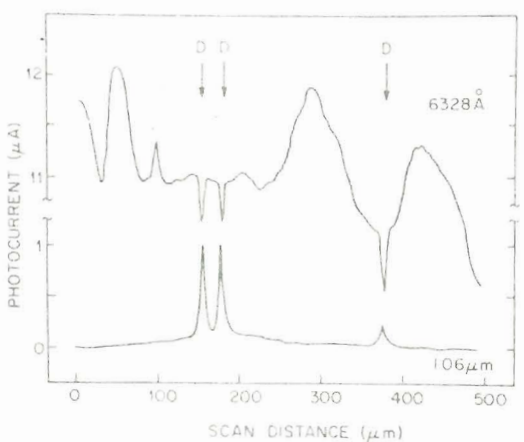

Fig. 2. Line scan across three dark lines (labeled D) which have been induced by catastrophic degradation of a $GaAs/Al_xGa_{1-x}As$ double heterostructure. The upper trace shows the decrease in collected photocurrent for an above-band-gap laser (6328 Å), while the lower trace shows the extrinsic photocurrent generated at the defects by a sub-band-gap laser (1.06 μm).

The second example, of a classic (100) DLD, is shown in Fig. 3. This is a photocurrent image of a (100) DLD obtained by scanning a focussed 1.06 μm laser beam in the plane of the DH laser active region after entering the sample through a window in the n-type ohmic contact and passing *through* the GaAs substrate. The two parallel, vertical bright lines in the image correspond to photocurrent generated at deep levels in the proton-bombarded regions which define the lasing stripe. They appear as narrow stripes because the horizonal scan was terminated after just reaching these regions. The series of irregular bright features in the center of the figure, which cross the lasing stripe at an angle, is the (100) DLD. Note the extremely good resolution, which is on the order of 1 μm. This is the maximum that one would have expected with light of 1.06 μm wavelength.

5. COMPARISON WITH OTHER METHODS OF RECOMBINATION MICROSCOPY

We mentioned in the introduction several other methods of recombination microscopy which also provide information about the spatial distribution of nonradiative recombination centers. Let us briefly discuss here the merits of the scanning *extrinsic* photocurrent (SEP) method relative to these other techniques.

First, SEP should not be viewed as a *replacement* for any of the other techniques, but rather a *complementary* measurement. It cannot replace the minority-carrier-lifetime-sensitive techniques, such as EBIC and above-band-gap photocurrent, since they are the ultimate measure of whether or not a particular defect is a recombination center. However, it is possible for these techniques to indicate reduced current at a microscopic short-circuit of the junction or at a location where an opaque defect lies between the junction and the surface and blocks the scanning beam. In these cases the SEP measurement should show *nothing* and thus verify that the reduced minority-carrier collection is not due to recombination at deep levels. Also in cases where the minority-carrier collection is reduced to near zero by a large concentration of recombination centers, SEP is a better measure of the defect concentration since there is essentially no limit to how *large* the SEP signal may be.

When compared to SEM charge collection measurements, the scanning laser technique (both above- and below-band-gap) has the obvious advantage of simplicity with very nearly the same resolution. In the below-gap scanning laser case the resolution is limited by the laser wavelength, in the SEM EBIC or cathodoluminescence case the resolution is limited by the carrier diffusion lengths. For many systems these are both on the order of a few μm.

It is perhaps most relevant, however, to compare the defect optical-emission SEP method with the defect thermal-emission SDLTS technique, since both attept to measure the energy level of the defect. A major difference, apart from the obvious fact that one is a thermal technique while the other is optical, is that the sensitivity of SDLTS is a strong function of the resolu-

tion. In fact, the SDLTS sensitivity is inversely proportional to the *square* of the resolution. Thus it is rather insensitive at its maximum reported resolution of $=2\ \mu$m[16]. The sensitivity of SEP, on the other hand, is *independent* of resolution, and furthermore may be increased without loss of resolution by using a more intense scanning laser beam, provided one does not enter the high-intensity limit where the resolution is controlled by the carrier diffusion length. A further advantage of SEP is that it can detect unsaturable minority-carrier traps, which neither DLTS or SDLTS can do. In addition, SEP can form an image of a junction plane located *deep* within the sample. Samples can also be examined with only pressed-on contacts. Good ohmic contacts are not required, as they are for SDLTS. On the other hand, the energy-level-measurement capabilities of SEP are not as good as SDLTS since the steady state photocurrent lineshapes are rather broad and difficult to interpret. In summary, we feel that none of the techniques of recombination microscopy has such a clear-cut advantage so as to be the method of choice. All measurements add valuable information and insight to the problem. The scanning extrinsic photocurrent method should be another very valuable tool to add to this class of measurement techniques.

Acknowledgements—The authors would like to thank F. R. Merritt for technical assistance and R. A. Logan and R. L. Hartman for providing the samples used to illustrate the technique.

REFERENCES

1. P. Petroff and R. L. Hartman, *Appl. Phys. Lett.* **23**, 469 (1973).
2. P. Petroff, W. D. Johnston, Jr. and R. L. Hartman, *Appl. Phys. Lett.* **25**, 226 (1974).
3. S. O'Hara, P. W. Hutchinson and P. S. Dobson, *Appl. Phys. Lett.* **30**, 368 (1977).
4. P. M. Petroff, L. C. Kimerling and W. D. Johnston, Jr., In *Radiation Effects in Semiconductors* 1976 (Inst. Phys. Conf. Serv. No. 31, Inst. Phys., London, 1977), p. 362.
5. B. C. DeLoach, B. W. Hakki, R. L. Hartman and L. A. D'Asaro, *Proc. IEEE* **61**, 1042 (1973).
6. W. D. Johnston, Jr. and B. I. Miller, *Appl. Phys. Lett.* **23**, 192 (1973).
7. W. Heinke and H. J. Queisser, *Phys. Rev. Lett.* **33**, 1082 (1974).
8. S. Metz, *Appl. Phys. Lett.* **30**, 296 (1977).
9. L. C. Kimerling, H. J. Leamy, J. L. Benton, S. D. Ferris, P. E. Freeland and J. J. Rubin, In *Semiconductor Silicon*, p. 468. Electrochem. Soc., Princeton, New Jersey (1977).
10. P. D. Dapkus and C. H. Henry, *J. Appl. Phys.* **47**, 4061 (1976).
11. P. M. Petroff, D. V. Lang, J. L. Strudel and R. A. Logan, *Scanning Electron Microscopy* Vol. 1, p. 325. SEM. Inc., AMF O'Hare, Ill. (1978).
12. T. H. DiStefano, *J. Appl. Phys.* **44**, 527 (1973).
13. T. H. DiStefano, *NBS Special Pub.* 400-23, ARPA/NBS Workshop IV. Surface Analysis for Silicon Device, Gaithersburg, Maryland, April 23–24 (1975).
14. C. H. Henry and R. A. Logan, *J. Appl. Phys.* **48**, 3962 (1977).
15. D. V. Lang, *J. Appl. Phys.* **45**, 3023 (1974).
16. P. M. Petroff and D. V. Lang, *Appl. Phys. Lett.* **31**, 60 (1977).
17. C. T. Sah and A. F. Tasch, *Phys. Rev. Lett.* **19**, 69 (1967).
18. C. T. Sah, L. Forbes, L. L. Rosier and A. F. Tasch, *Solid State Electron.* **13**, 759 (1970).
19. S. Braun and H. G. Grimmeiss, *J. Appl. Phys.* **44**, 2789 (1973).
20. H. G. Grimmeiss, *Ann. Rev. Mat. Sci.* **7**, 341 (1977).
21. S. M. Sze, *Physics of Semiconductor Devices*, p. 640. Wiley, New York (1969).
22. C. H. Henry and D. V. Lang, *Phys. Rev. B.* **15**, 989 (1977).
23. *G*100 PD *optical scanner*, General Scanning, Inc.
24. C. H. Henry, P. M. Petroff, R. A. Logan and F. R. Merritt, *J. Appl. Phys.* (to be published).